J Nanostruct 16(2): 2595-2606, Spring 2026

RESEARCH PAPER

Graphene-based Nanocomposite Containing Au, Sb, and Si to Enhance the Sensitivity of Carbon-monoxide and Ammonia Gas Sensors

*Marziyeh Azami, Fatemeh Pakpour *, Davood Ghanbari*

Department of Science, Arak University of Technology, Arak, Iran

ARTICLE INFO

Article History:
Received 22 December 2025
Accepted 15 March 2026
Published 01 April 2026

Keywords:
Ammonia
Carbon monoxide
Gas sensor
Graphene-based sensors
Nanocomposites

ABSTRACT

Carbon monoxide (CO) and ammonia (NH_3) are highly toxic gases that pose serious health risks. The development of gas sensors capable of detecting low concentrations of these gases at room temperature is therefore of great importance. In this work, we report the synthesis and characterization of graphene-based nanocomposites modified with gold (Au), antimony oxide (Sb_2O_3), and silica (SiO_2), focusing on steady-state sensing response and recovery process toward CO and NH_3. For the synthesis of graphene oxide (GO), a modified Hummers' method was applied. Gold, antimony trioxide, and silica nanoparticles were prepared through hydrothermal, sonochemical, and sol-gel methods, respectively. The structural and morphological properties of as-prepared nanostructures were investigated using SEM, XRD, FT-IR, EXD, and MAP Analysis. Gas sensing tests reveal that the nanocomposites exhibit significantly improved sensitivity to both CO and NH_3, with lower detection limits, sharper response and recovery times compared to pure graphene oxide. As the best result, GO/Au showed a 60% change in response time to CO and around a 42% change to NH3, in addition to improvements of 52% for recovery time from CO gas and 54% from NH3 gas, compared to pure GO. These findings suggest that all three nanocomposites present a promising pathway toward high-performance, room-temperature CO and NH_3 sensors, with the GO/Au nanocomposite offering an advantage.

How to cite this article
Azami M., Pakpour F., Ghanbari D. Graphene-based Nanocomposite Containing Au, Sb, and Si to Enhance the Sensitivity of Carbon-monoxide and Ammonia Gas Sensors. J Nanostruct, 2026; 16(2):2595-2606. DOI: 10.22052/JNS.2026.02.098

INTRODUCTION

Toxic gases such as carbon monoxide (CO) and ammonia (NH_3) pose serious health and safety risks. CO is a colorless and odorless gas that is mainly produced by the incomplete combustion of almost any carbon-containing material and fossil fuels. Even a low concentration of CO can disturb oxygen transport in the body, leading to neurological damage or death [1]. $NH_3$is another toxic gas that is commonly produced by industrial and agricultural activities, has irritating and corrosive properties, and can damage the eyes, lungs, and other organs [2]. Ammonia is a gas found everywhere, produced naturally in soils. Its source is the metabolism of bacteria and the breakdown of dead plants, animals, and animal waste. Since NH_3 plays a key role in the nitrogen cycle, it is a normal part of the soil, air, and water

* *Corresponding Author Email: f.pakpour@arakut.ac.ir*

This work is licensed under the Creative Commons Attribution 4.0 International License.
To view a copy of this license, visit http://creativecommons.org/licenses/by/4.0/.

in the natural environment [3]. Every year, many fatalities and health issues result from exposure to these gases, particularly in environments with poor ventilation or industrial incidents. Thus, highly sensitive, selective, and reliable gas sensors are critically needed to detect CO and NH_3 at low concentrations, ideally under ambient conditions.

Current traditional gas sensors, which mainly use metal oxide semiconductors and polymer materials, use optical, calorimetric, gas chromatography, and acoustic sensing methods. However, these sensors often have several limitations, such as high cost and high-power consumption [4]. As a better alternative, nanomaterial-based gas sensors are rapidly gaining popularity. Their unique electrical, optical, and thermal properties, combined with their large surface area relative to their size, allow for superior performance, offering quick response and recovery times, high sensitivity and selectivity, and enhanced stability [5].

More recently, graphene and its related materials such as pristine graphene, graphene oxide (GO), and reduced graphene oxide (RGO) have captured attention for gas sensing thanks to their remarkable properties including high mechanical strength, thermal ballistic conductivity, high electron mobility, low electrical noise, and a large surface area due to their unique two-dimensional structure [6-10]. The most critical feature making graphene a promising candidate for gas sensing is its high sensitivity down to a single molecule. The electronic properties of graphene change upon absorbing gas molecules onto its surface.

Pristine graphene is a zero-bandgap semimetal with extremely high carrier mobility and conductivity [11] with a defect-free sp2 carbon lattice. It provides only weak adsorption sites [12] and shows a small resistance change upon exposure to gas molecules [13]. Intrinsic graphene also lacks the necessary functional groups for breaking the perfect sp^2 lattice and creating localized electronic states. It is also not producible on a large scale. Graphene oxide, on the other hand, exhibits chemiresistive behavior primarily due to its heterogeneous structure and abundant oxygen-containing functional groups, hydroxyl, epoxy, carbonyl, and carboxyl, which break the extended π-network, introduce a tunable bandgap, and create a high-resistance semiconducting baseline [14]. These functional groups serve as chemically active adsorption sites, enabling strong interactions with analytes and significant charge-transfer-induced modulation of conductivity [15]. Although GO exhibits a much larger chemiresistive response than pristine graphene, it suffers from humidity cross-sensitivities and long-term signal drift, and limited selectivity toward specific gases. To overcome these drawbacks in graphene-based sensors, scientists use techniques like doping, hybridization, and functionalization [7]. Modifications of graphene via doping, defect engineering, or decoration with nanoparticles are known to improve both sensitivity and selectivity, and response dynamics [16]. Despite the advances, there are still gaps. Many sensors perform well for either NH_3 or CO, but less research has studied a sensor that demonstrates simultaneous high sensitivity to both gases, while also maintaining stability, response, and recovery times under ambient conditions.

Incorporation of gold (Au), antimony (Sb), and silicon (Si) into GO will synergistically enhance its chemiresistive response toward CO and NH_3 gases. Each dopant contributes a distinct, experimentally established function that is beneficial for gas sensing. Gold nanoparticles act as catalytic sites that increase the interaction between GO and gas molecules, promote charge transfer, enhance the sensitivity of GO, and accelerate response–recovery kinetics of the sensor [20,21]. Antimony doping modifies the electronic properties of GO, introduces structural defects, and stabilises oxygen-related adsorption sites, leading to a higher sensitivity and stability of the sensor. On the other hand, Sb reduces interference from ambient moisture and increases thehumidity tolerance of the sensor [22,23]. Silicon is typically introduced in the form of SiO_2 nanoparticles, which create a three-dimensional porous networkand increase the effective surface area and active adsorption sites on GO [24]. Additionally, Si-based structures help to uniformly disperse metal nanoparticles, preventing aggregation and ensuring that catalytic sites remain accessible, which improves the reproducibility and stability of the sensor [25]. Si can also modulate the local electronic environment of GO, optimising charge-transfer interactions between adsorbed gas molecules and the sensing layer, leading to amplifying the chemiresistive response [26]. Together, these effects contribute to improved sensitivity, faster response and recovery times, and improve long-

CC BY

term stability of GO-based gas sensors.

In this work, we explore graphene-based nanocomposites containing gold, antimony, and silicon as modifiers to enhance gas sensing performance toward CO and NH_3. We report the synthesis, structural and electronic characterization, and the gas sensing behavior (sensitivity, detection limit, response, and recovery) of GO/Au, GO/Sb_2O_3, and GO/SiO_2nanocomposites at room temperature.

This research aims to contribute to lower detection limits for CO and NH_3, better steady state response, and recovery time at room temperature. By doing so, the study may advance the development of more effective gas sensor materials to help reduce pathogenesis and mortality from toxic gas exposure.

MATERIALS AND METHODS

Materials

In this research, graphite, sulfuric acid, phosphoric acid, potassium permanganate, hydrogen peroxide, hydrochloric acid, gold, antimony trioxide, and silica nanoparticles were used, all purchased from Merck company (Germany) with a high purity of above 99%. Deionized double-distilled water was used throughout the experimental procedures. XRD analysis was performed using an X'Pert-Pro device made by Philips (Netherlands), which enables qualitative phase identification and is supported by the X'PertHighScore software for detailed phase analysis. SEM imaging was carried out with a MIRA TESCAN instrument equipped with a high-resolution Schottky emitter, providing high-quality, low-noise images. FT-IR spectra were recorded using a Spectrum 2 manufactured by PerkinElmer Company.

Synthesis of GO

Graphene oxide was synthesized using the modified Hummers method. First, 3 g of graphite powder was added to 360 mL of sulfuric acid and 40 mL of phosphoric acid (ratio 9:1) in a beaker, and the solution was stirred slowly with a magnetic stirrer at room temperature. Then, 18 g of potassium permanganate was slowly added to the mixture to avoid an explosion. As the reaction is exothermic, once the temperature reached 35–40 °C, the beaker was transferred to an oil bath at 50 °C and stirred continuously for 12 hours. The reaction vessel was removed from the bath and allowed to cool to room temperature. To quench residual potassium permanganate, 400 mL of ice water at 0°C and 3 mL of hydrogen peroxide were added under the hood, resulting in a yellow-colored suspension. The mixture was centrifuged, and the collected solids were washed with 200 mL of double-distilled water. Repeat the centrifugation and again wash with 200 mL of hydrochloric acid, followed by washing with 200 mL of ethanol. These washing steps were performed to remove residual metal ions and acids, and to achieve a neutral pH. Finally, the purified product was dried in an oven at 80 °C, yielding the synthesized graphene oxide.

Synthesis of nanoparticles

Gold nanoparticles were synthesized using a hydrothermal method. First, 0.3 g of gold (III) chloride ($AuCl_3$) was dissolved in 200 mL of deionized water and stirred for 5 minutes. Then, 0.5 g of sodium citrate ($Na_3C_6H_5O_7$) was added as a reducing and stabilizing agent, and the mixture was stirred for an additional 30 minutes. The solution was transferred to an autoclave and heated at 200 °C for 5 hours. After cooling, the resulting precipitate was washed with 200 mL of distilled water and ethanol, then separated by centrifugation at 3000 rpm for 5 minutes. The final product was dried in an oven at 86 °C.

Antimony trioxide nanoparticles were synthesized using a sonochemical approach. In a beaker, 1 g of antimony (III) chloride ($SbCl_3$) was dissolved in 100 mL of ethylene glycol ($C_2H_6O_2$) and stirred for 5 minutes. Subsequently, 10 mL of 1 M ammonia solution was added to induce precipitation, followed by 30 minutes of stirring. The mixture was then subjected to ultrasonic irradiation at 150 W for 60 minutes. The resulting precipitate was collected by centrifugation, washed with 200 mL of distilled water and ethanol, and centrifuged again at 3000 rpm for 5 minutes. The final precipitate was dried at 60 °C.

Silica nanoparticles were synthesized via a sol–gel method. First, 1 g of tetraethoxysilane (TEOS) was dissolved in 20 mL of ethylene glycol ($(CH_2OH)_2$) and stirred for 5 minutes. Then, 10 mL of 1 M ammonia solution was added as a catalyst and precipitating agent. The mixture was stirred under a fume hood at 200 °C for 2 hours, during which it gradually formed a gel. The gel was transferred to a crucible and heated in an oven at 500 °C for 2 hours, then allowed to dry slowly at room temperature.

CC BY

Preparing nanocomposites

To prepare the graphene oxide/gold nanocomposite (GO/Au), 0.1 g of graphene oxide was dissolved in 100 mL of deionized double-distilled water and dispersed using an ultrasonic device with a power of 500 W for 60 minutes. Separately,0.05 g of gold nanoparticles was dissolved in 100 mL of deionized double-distilled water and dispersed using an ultrasonic device with a power of 500 W for 60 minutes. The gold colloid was added to the graphene oxide solution and treated under ultrasonic waves with a power of 1000 W for 30 minutes. The resulting suspension sample was stirred for 5 hours at 70 °C on a magnetic stirrer, and finally it was separated by centrifugation at 5000 rpm and dried in an oven. The same procedure with the same amount of materials was applied for preparing GO/Sb_2O_3 using GO and Sb_2O_3 nanoparticles, and GO/SiO2 using GO and SiO_2 nanoparticles.

Sensorial test setup and measurement

To check the sensing properties of the samples, a chamber was built with an inlet valve at the top of the chamber for gas injection and an outlet valve at the bottom of the chamber for gas discharge, and to prevent the concentration of the gas in the chamber from reaching full saturation. The inlet valve was connected to a needle pressure gauge to control the inlet gas pressure. A fan was used for better circulation of gas inside the chamber. The inlet valve is connected to a regulator, and the regulator is also connected to the capsule containing toxic gas. The samples were formed into tablets using a tablet press machine and placed in their special location in the experimental setup, and connected to a four-point probe resistivity measurement device. A schematic of the testing setup is shown in Fig. 1.

As Carbon monoxide is an n-type gas that is an electron donor, it has a pair of non-bonding electrons. Like many semiconductor gas sensors, the sensitivity of gas sensors made of graphene oxide sheets is based on surface adsorption. The sensing mechanism involves the surface conductivity being modulated by the adsorbed gas molecules. The electrical conductivity is strongly dependent on the surface states produced by the molecular adsorption, which leads to a charge space between the layers. The sensing is more specifically related to the adsorption of oxygen species, water ions, or hydroxyls, which act as mediators and catalyze the charge transfer process. The oxygen groups in graphene oxide are responsible for the chemical reaction with the C-O bond with the gas molecules. The hydroxyl groups in graphene oxide increase the number of conduction band electrons, resulting in an enhanced depletion layer.

CO gas adsorbed on the surface of GO creates moisture, which has a positive effect on the sensor. When the sensor is exposed to CO gas, reduction reactions occur between CO gas and hydroxyl and oxygen groups, releasing electrons that neutralize

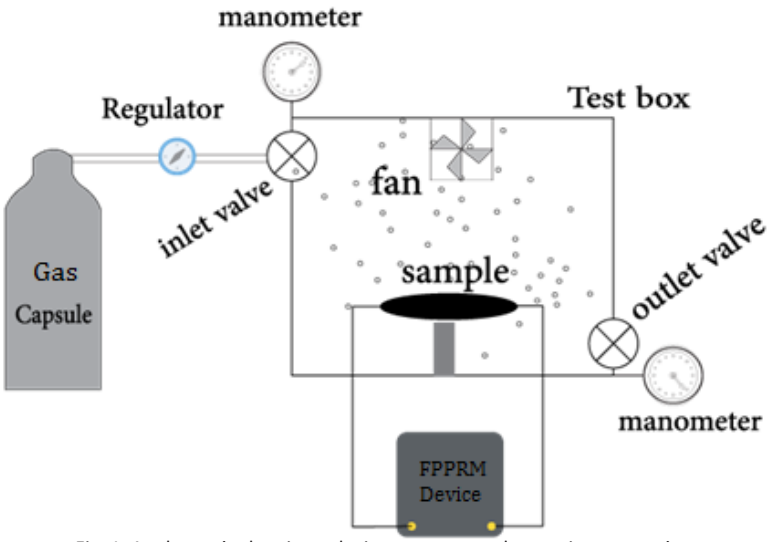


Fig. 1. A schematic showing a device to measure the sensing properties.

holes, and the products of this reaction are carbon dioxide and water. The hydroxyl groups in GO are responsible for the production of CO_2 and H_2O through the following chemical reaction:

$2OH^- + CO \rightarrow CO + H_2O + 2e^-$

On the other hand, the surface adsorption of oxygen species in the nanocomposites is responsible for the production of CO_2 and electrons:

$O_2^- + 2CO \rightarrow 2CO_2 + 2^-$

These released electrons neutralize the holes, thus reducing the holes of accumulation layer and the electrical conductivity decreases as a function of time, thus leading to an increase in the resistance of the sensor [21].

To calculate the sensor response time, we use

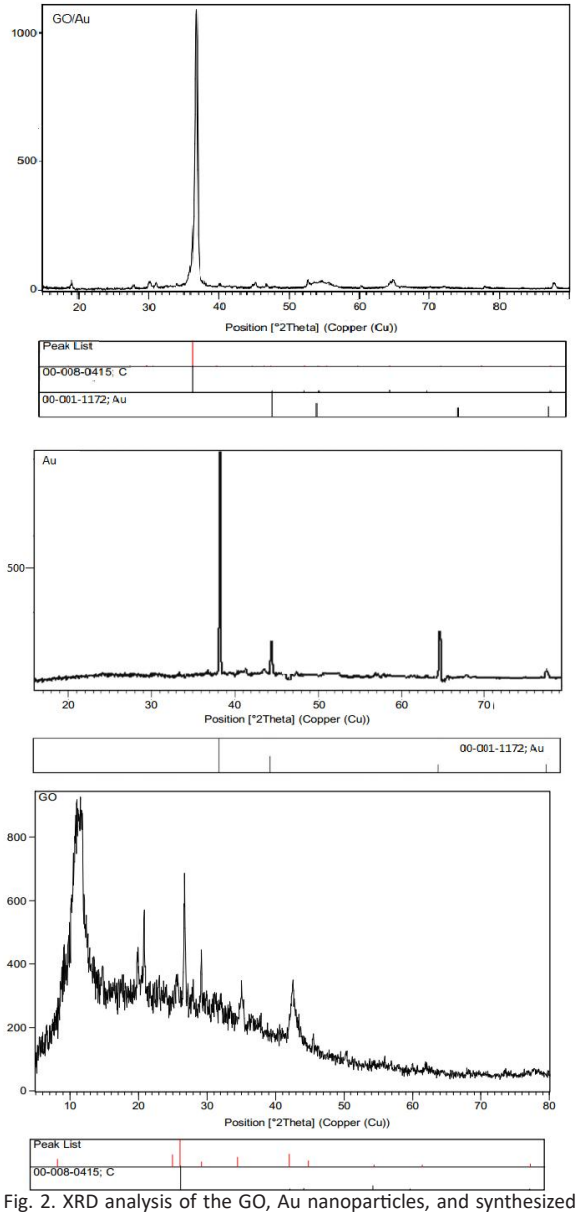


Fig. 2. XRD analysis of the GO, Au nanoparticles, and synthesized GO/Au nanocomposite. The peak in angle 2q between 20 and 30 degrees in the GO/Au pattern is associated with gold particles.

(cc) BY

the following relationship:

$$\text{Response}\ (\%) = \frac{R_{gas} - R_{air}}{R_{air}} \times 100 \quad (1)$$

where R_{gas} is the resistance of the sample in the presence of CO or NH_3 gas, and R_{air} is the resistance of the sample in normal air.

To analyze the sensor recovery results, we use the following relationship:

$$\text{Recovery}\ (\%) = \frac{R_{gas} - R_{sat}}{R_{sat}} \times 100 \quad (2)$$

where here R_{sat} is the resistance of the sample in the saturated state.

RESULTS AND DISCUSSION

Characterization

Fig. 2 shows the XRD analysis for GO, Au nanoparticles, and GO/Au nanocomposite. The characteristic peaks at the angle (2θ) with sizes of 38.26, 44.6, 64.68, and 77.54 in the XRD pattern of Gold correspond to (111), (200), (220), and (311) planes. The crystal structure of the nanoparticles has a cubic phase with the space group Fm-3m with the number 255. The average crystal size was calculated to be about 55 nm using the Debye-Scherrer equation. The sharp peak in the XRD pattern of GO/Au at 2q between 20 and 30 degrees is associated with the presence of gold nanoparticles in the GO network.

Fig. 3 shows SEM, MAP, FT-IR, and EDX analyses for GO/Au nanocomposites. As it is seen from the SEM, the nanoparticles did not agglomerate at the nanoscale, and the average particle size is around 28 nm. In MAP analysis, the green dots are associated with carbon, the purple dots are associated with oxygen, and the blue dots are associated with gold elements. In the FT-IR

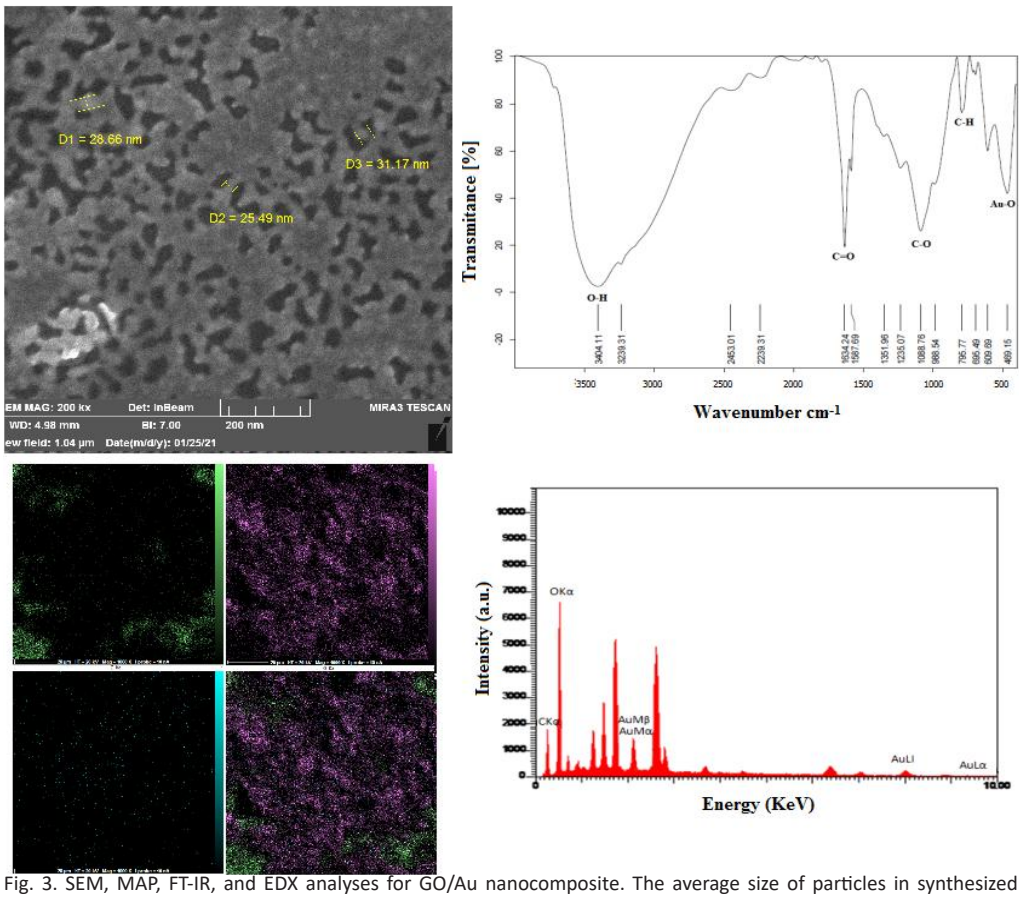


Fig. 3. SEM, MAP, FT-IR, and EDX analyses for GO/Au nanocomposite. The average size of particles in synthesized composites, according to SEM, is around 28 nm. The green dots in MAP analysis are related to carbon, the purple dots are related to oxygen, and the blue dots are associated with gold.

CC BY

image, the broad peak at 3404 cm^{-1} is related to the hydroxyl group (O-H) adsorbed on the GO/Au nanocomposite. The absorption peak at 1634 $cm^{-1}$is related to the asymmetric stretching vibration of the carboxyl bonds (C=O). The absorption peak at 1088 cm^{-1} is related to the stretching band of the carbon-oxygen single bond (C-O). The absorption peak at 795 cm^{-1} is related to the bending band of the carbon-hydrogen (C-H) bond. The absorption in the region of 469 cm^{-1} is related to the stretching vibrations of gold-oxygen (Au-O) bonds. The EDX elemental analysis spectrum of the GO/Au nanocomposite confirms the presence of carbon, oxygen, and gold elements. The Kα peak is related to carbon element with the energy 0.26 keV, and the Kα peak corresponding to oxygen element with energy of 0.7 keV in this spectrum. The Mα and Mβ peaks with an energy of 2.63 keV are related to gold. The LI and Lα peaks are also related to the gold element, which is created in the background of the spectrum.

Fig. 4 shows SEM, MAP, FT-IR, and EDX analyses for GO/Sb_2O_3 nanocomposites. SEM shows that the nanoparticles did not agglomerate at the nanoscale, and the average size of the particles is measured to be around 24 nm. In the MAP analysis, the green dots are related to carbon, the purple dots are related to oxygen, and the yellow dots are related to antimony elements. In the FT-IR analysis of GO/Sb_2O_3, the broad peak in the region of 3403 cm^{-1} is related to the hydroxyl (O-H) group adsorbed on the graphene oxide/ antimony trioxide nanocomposite. The absorption peak in the region of 1634 cm^{-1} is related to the asymmetric stretching vibration of the carboxyl bonds (C=O). The absorption peak in the region of 1088 cm^{-1} is related to the stretching band of the carbon-oxygen single bond (C-O). The absorption peak in the region of 796 cm^{-1} is related to the bending band of the carbon-hydrogen bond (C-H). The absorption in the region of 464 cm^{-1} is related to the stretching vibrations of the antimony-

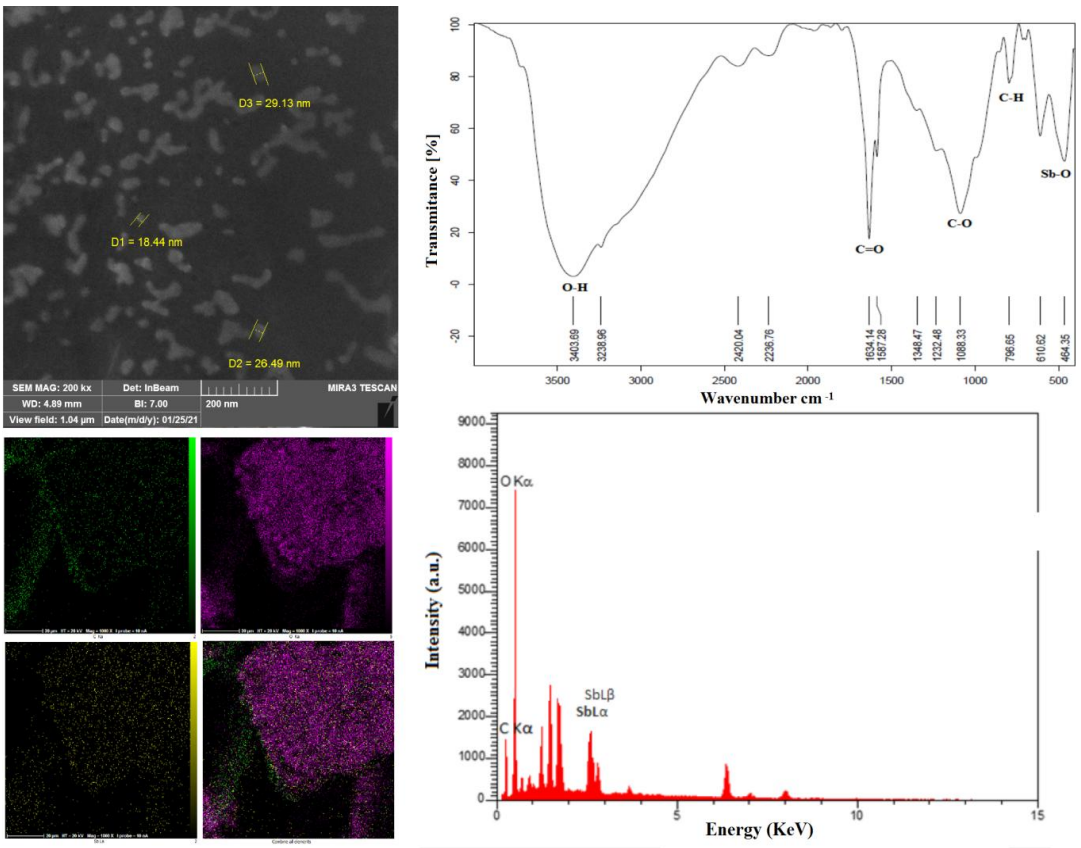


Fig. 4. SEM, MAP, FT-IR, and EDX analyses for GO/Sb_2O_3 nanocomposite. The average size of particles in synthesized composites, according to SEM, is around 24 nm. The green dots in the MAP analysis are related to carbon, the purple dots are related to oxygen, and the yellow dots are related to antimony elements.

CC BY

oxygen bonds (Sb-O). The EDX spectrum of GO/Sb2O3 nanocomposite proves the presence of carbon, oxygen, and antimony elements in the prepared nanocomposite. The Kα peak is related to the carbon with an energy of 0.22 keV, and the Kα peak is related to the oxygen with an energy of 0.51 keV. The Lα and Lβ peaks with an energy of 2.68 keV are related to the antimony element.

And finally, Fig. 5 illustrates the SEM, MAP, FT-IR, and EDX analyses for GO/SiO_2 nanocomposites. SEM shows that the porous silica nanoparticles are well-positioned on the surface of graphene oxide, and its nanopores can be seen in the image. The silica nanoparticles have a spherical and homogeneous morphology and are formed in a monodisperse form. The average size of the particles is measured to be around 31 nm. In the MAP image, the green dots are related to carbon, the purple dots to oxygen, and the blue dots are related to silicon.

In the FT-IR spectrum of the GO/SiO_2, the absorption peak in the region of 3669 cm^{-1} is related to the hydroxyl group (O-H) adsorbed on the GO/SiO_2nanocomposite. Also, the absorption peak in the region of 1611 cm^{-1} is related to the (C=O) double bonds. The absorption peak in the region of 1091 cm^{-1} is related to the stretching band of the carbon-oxygen single bond (C-O). The absorption peak in the region of 780 cm^{-1} is related to the bending band of the carbon-hydrogen bond (C-H). The absorption in the region of 475 cm^{-1}indicates the stretching vibrations of the silicon-oxygen bonds (Si-O). The EDX elemental analysis spectrum for GO/SiO_2 proves the presence of carbon, oxygen, and silica elements in the prepared nanocomposite.

Results of sensorial measurements

As mentioned, a setup similar to the one shown in Fig. 1 was used for the measurement of the sensorial properties of prepared sensors. The measurement was performed at 25 ˚C. The

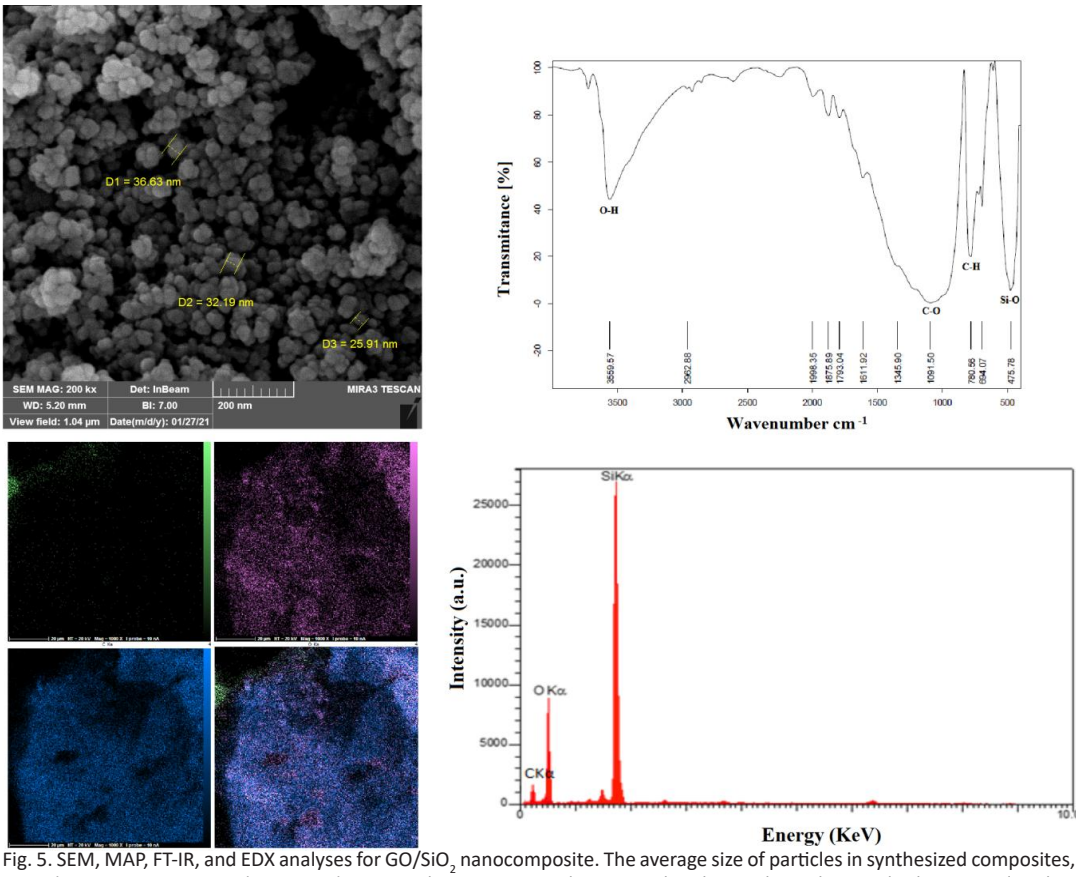


Fig. 5. SEM, MAP, FT-IR, and EDX analyses for GO/SiO_2 nanocomposite. The average size of particles in synthesized composites, according to SEM, is around 31 nm. The green dots in MAP analysis are related to carbon, the purple dots are related to oxygen, and the blue dots are related to silicon elements.

CC BY

injection of CO/NH_3 was done by the capsule, and the rate of gas injection was kept constant at 200cc/min for the measurement of response time. The concentration of CO inside the test environment was gradually increased from zero to 150 ppm. Due to the sensitivity of GO to moisture and water vapor, it is necessary to remove moisture from the surface of the tablet samples. For this purpose, first, a flow of nitrogen gas with a constant flow was introduced into the sensor chamber. Toxic gas was then introduced into the chamber with a constant flow, and the changes in the electrical resistance of the tablet were measured at each stage by a precise four-point probe resistance measuring device. Each measurement was repeated three times under the same conditions, and the average was calculated for plotting the graphs of sensor response according to equation (1).

The results of the response for all sensors upon introducing CO and NH_3 gas are presented in Figs. 6a and 6b, respectively. For pure GO, upon introducing CO gas, an increase in the electrical resistance of the sample was observed after 5 s. The sample resistance reached a saturation value in 42 s and remained constant after that. For NH_3, an increase in the electrical resistance was observed after 12 s and reached a plateau at around 37 s. With the same procedure as mentioned above, the response graphs were plotted for GO/Au, GO/Sb_2O_3, and GO/SiO_2 nanocomposites upon introducing CO and NH_3 gases. As it is seen, the onset of response to CO gas for GO/Au is at 2 s and reaches a plateau at 20 s. The onset of response for GO/Au in the presence of NH3 gas is about 7 s, and it reached the saturation value at 27 s. The onset of response for GO/Sb_2O_3 is 3 s for CO and 15 s for NH_3. And finally. The onset of response for GO/SiO_2 is 3 s for Co and 10 s for NH_3.

To investigate the reversibility of the sensor, a flow of nitrogen gas was introduced into the

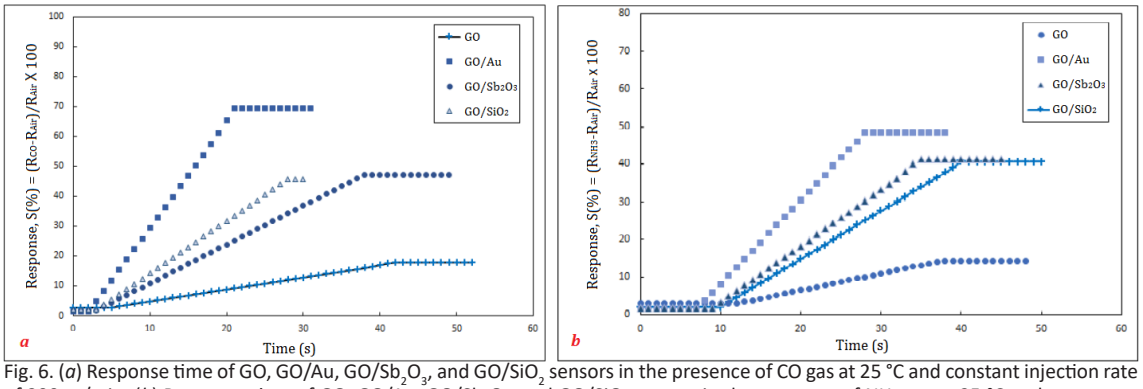


Fig. 6. (*a*) Response time of GO, GO/Au, GO/Sb_2O_3, and GO/SiO_2 sensors in the presence of CO gas at 25 °C and constant injection rate of 200 cc/min. (*b*) Response time of GO, GO/Au, GO/Sb_2O_3, and GO/SiO_2 sensors in the presence of NH_3 gas at 25 °C and a constant injection rate of 200 cc/min.

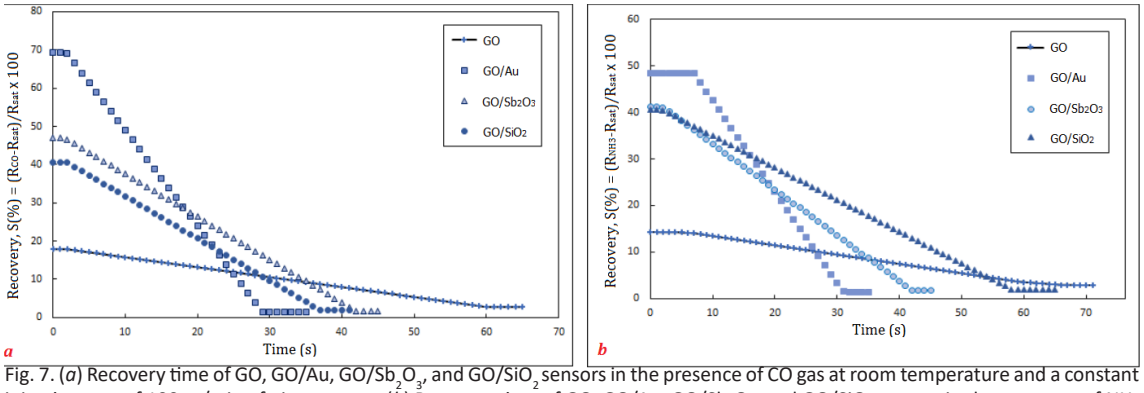


Fig. 7. (*a*) Recovery time of GO, GO/Au, GO/Sb_2O_3, and GO/SiO_2 sensors in the presence of CO gas at room temperature and a constant injection rate of 100 cc/min of nitrogen gas. (*b*) Recovery time of GO, GO/Au, GO/Sb_2O_3, and GO/SiO_2 sensors in the presence of NH_3 gas at room temperature and a constant injection rate of nitrogen at 100 cc/min.

CC BY

chamber to clean the sample surface from CO or NH_3 gas. As the nitrogen gas entered, the sensor resistance decreased and finally reached the base resistance. The average percentage of changes in the sensor recovery time after removing CO gas is shown in Fig. 7a, and for NH_3 gas is shown in Fig. 7b. The GO sensor, after removing CO gas, reaches the base resistance in 60 s, and after removing NH_3 in 65 s. For GO/Au, this recovery time is 27 s for CO gas and 31 s for NH_3. The GO/Sb_2O_3 sensor is recovered after 42 s for both gases. And finally, GO/SiO_2 is recovered after 36 s for CO and 58 s for NH_3.

The key parameters of sensing behavior for each nanocomposite and in the presence of each gas, such as the Response (sensitivity), response time, and recovery time, are summarized in Table 1. The sensor's response time, defined as the time required to reach 63.2% of the final response, was estimated based on interpolation of the Response (%) vs. time curves.

As seen in the results of sensorial measurements for pure GO in the presence of CO gas, a change in electrical resistance occurs. The presence of oxygen-containing functional groups in graphene oxide makes its surface favorable for gas absorption, and gas molecules are adsorbed on defect sites and these functional groups. The behavior of graphene oxide is P-type, that is, it is an electron acceptor. CO gas is adsorbed on the surface of the graphene oxide sample and changes the concentration of charge carriers on its surface, leading to a decrease in electrical conductivity.

Doping the graphene oxide with gold nanoparticles increases the gas detection capability of the sensor due to the catalytic property of gold and the high surface-to-volume ratio of graphene oxide and gold nanoparticles. In fact, by absorbing gas on the surface of the sample, the conduction paths are reduced, and the resistance increases. The use of gold as a conductive phase improves the sensor response and catalyzes the charge transfer process.

The modified GO sample by antimony trioxide nanoparticles increases the conductivity of the sample. The catalytic property of antimony trioxide and its high surface-to-volume ratio increase the gas detection capability. Also, the synergistic effect of GO and Sb_2O_3 increased the porosity of the sample. Carbon monoxide reducing gas, transfers its electron pair to the GO/Sb_2O_3 sample, causing electrons to be placed in the holes and reducing the conduction paths, which increases the electrical resistance.

Regarding recovery time, with the exit of nitrogen gas, the surface of the GO/Sb_2O_3 sample was cleaned of carbon monoxide gas. Given that gas absorption on the surface of the sample occurs by weak van der Waals forces, with the entry of nitrogen gas, the sensor resistance decreases and approaches the base resistance. The sample resistance reaching the initial value indicates the reversibility of the sensor. Carbon monoxide reducing gas transfers its electron pair to the GO/SiO_2 tablet, causing electrons to be placed in the nanopores and reducing the conduction paths, which increases the electrical resistance. The recovery time for GO/Sb_2O_3 is longer than that of the GO/SiO_2 and is probably due to the greater porosity of the GO/SiO_2 tablet and the placement of more gas molecules on the sample surface.

The test results on the four graphene-based sensors show that these sensors have a good detection capability for CO and NH_3 gases. The response time for all samples in the presence of CO gas is below 1 minute, with a very significant

Table 1. Comparison of the properties of fabricated sensors. The best values for each are marked in green. The operating temperature is 25 °C. The rate of gas injection is 200 cc/min and the final value of gas concentration is 150 ppm. The last column shows some from the previous studies of graphene-base sensors from references [16,18,29].

	Sensor	GO	GO/Au	GO/Sb_2O_3	GO/SiO_2	Data from literature [16,18,29]		
						Pristine G (400 ppt)	functionalized rGO film	ZnO–rGO (1 ppm)
Response (sensitivity) (%)	CO	18	70	47	45	-	44 (10 ppm)	-
	NH_3	15	50	40	40	0.005	7 (100 ppm)	24.0
Response time (s)	CO	30.6	14.4	23.8	18.8	-	-	-
	NH_3	27.9	20.8	27.9	28.9	300	-	-
Recovery time (s)	CO	60	29	42	36	-	-	-
	NH_3	67	31	42	58	-	-	-

CC BY

result for GO/Au, at about 14.4 s for CO and 20.8 s for NH_3. The results for other sensors are also promising which showing a significant improvement in contrast to pure GO. A very good improvement is seen in recovery time for the GO/Au sensor in comparison to pure GO, and a moderate improvement in both other nanocomposites.

To further contextualize the performance of the synthesized nanocomposite sensors, Table 1 compares the key sensing parameters—including sensitivity, response, and recovery time with previously reported graphene-based or metal-oxide composite sensors from the literature [16, 18]. As shown, the GO/Au sensor exhibits the fastest response to CO and a markedly shorter recovery time compared to pristine graphene and to benchmark materials, which we attribute to the catalytic activity and charge-transfer efficiency of Au nanoparticles. Meanwhile, GO/Sb_2O_3 displays enhanced sensitivity and a balanced response–recovery behavior due to the synergistic interaction between Sb_2O_3 domains and the graphene matrix. The GO/SiO_2 sensor also outperforms pristine graphene in both gases, benefiting from increased porosity and surface accessibility. Overall, the comparison demonstrates that our modified nanocomposites—particularly GO/Au and GO/Sb_2O_3—provide competitive or superior performance relative to state-of-the-art room-temperature CO and NH_3 sensors, further confirming their potential for practical environmental monitoring applications.

CONCLUSION

In conclusion, in this research, GO, GO/Au, GO/Sb_2O_3, and GO/SiO_2 were successfully synthesized. According to the analyses performed on the prepared samples, nanocomposites were successfully placed in the nanometer phase. The structural and morphological analyses confirm the uniform distribution of Au nanoparticles, Sb_2O_3 domains, and SiO_2 modifier phases over the graphene matrix, creating abundant active sites and facilitating charge transfer. Gas sensing tests reveal that the composite exhibits significantly improved sensitivity to both CO and NH_3, sharper response and recovery times in comparison to non-modified graphene oxide. This study presents a promising pathway toward high-performance, room-temperature CO and NH_3 graphene-based sensors, which may be beneficial for environmental monitoring and public health applications.

CONFLICT OF INTEREST

The authors declare that there is no conflict of interests regarding the publication of this manuscript.

REFERENCES

1. Penney D. Chronic Carbon Monoxide Poisoning. Carbon Monoxide Toxicity: CRC Press; 2000. p. 393-418. http://dx.doi.org/10.1201/9781420039320.ch18
2. Spector O, Jacobson E. Advanced ammonia (NH_3) monitoring system for industrial applications. SPIE Proceedings; 1999/12/21: SPIE; 1999. p. 233-238.
3. M. Hizam SM, Al-Dhahebi AM, Mohamed Saheed MS. Recent Advances in Graphene-Based Nanocomposites for Ammonia Detection. Polymers. 2022;14(23):5125.
4. Liu X, Cheng S, Liu H, Hu S, Zhang D, Ning H. A Survey on Gas Sensing Technology. Sensors. 2012;12(7):9635-9665.
5. Jiménez-Cadena G, Riu J, Rius FX. Gas sensors based on nanostructured materials. The Analyst. 2007;132(11):1083.
6. Lu G, Yu K, Ocola LE, Chen J. Ultrafast room temperature NH3 sensing with positively gated reduced graphene oxide field-effect transistors. Chem Commun. 2011;47(27):7761.
7. Gupta Chatterjee S, Chatterjee S, Ray AK, Chakraborty AK. Graphene–metal oxide nanohybrids for toxic gas sensor: A review. Sensors Actuators B: Chem. 2015;221:1170-1181.
8. Kiranakumar HV, Thejas R, Naveen CS, Khan MI, Prasanna GD, Reddy S, et al. A review on electrical and gas-sensing properties of reduced graphene oxide-metal oxide nanocomposites. Biomass Conversion and Biorefinery. 2022;14(12):12625-12635.
9. Korucu Ş, Kose A, Fellah MF. Pt, Pd and Au decorated reduced graphene oxide: Sensing properties for phenol gas detection at room temperature. Synth Met. 2024;306:117623.
10. Mirahsani SF, Pakpour F, Ghanbari D. Graphene-Based Nanocomposite Containing Bismuth-Tin Oxide for Increasing the Efficiency of Carbon-Monoxide Sensors. Journal of Inorganic and Organometallic Polymers and Materials. 2024;35(6):4417-4431.
11. Novoselov KS, Geim AK, Morozov SV, Jiang D, Zhang Y, Dubonos SV, et al. Electric Field Effect in Atomically Thin Carbon Films. Science. 2004;306(5696):666-669.
12. Schedin F, Geim AK, Morozov SV, Hill EW, Blake P, Katsnelson MI, et al. Detection of individual gas molecules adsorbed on graphene. Nature Materials. 2007;6(9):652-655.
13. Yavari F, Koratkar N. Graphene-Based Chemical Sensors. The Journal of Physical Chemistry Letters. 2012;3(13):1746-1753.
14. Dreyer DR, Park S, Bielawski CW, Ruoff RS. The chemistry of graphene oxide. Chem Soc Rev. 2010;39(1):228-240.
15. Eda G, Chhowalla M. Chemically Derived Graphene Oxide: Towards Large-Area Thin-Film Electronics and Optoelectronics. Adv Mater. 2010;22(22):2392-2415.
16. Sun D, Luo Y, Debliquy M, Zhang C. Graphene-enhanced metal oxide gas sensors at room temperature: a review. Beilstein Journal of Nanotechnology. 2018;9:2832-2844.
17. Lerf A, He H, Forster M, Klinowski J. Structure of Graphite Oxide Revisited. The Journal of Physical Chemistry B. 1998;102(23):4477-4482.
18. Recum P, Hirsch T. Graphene-based chemiresistive gas sensors. Nanoscale Advances. 2024;6(1):11-31.

CC BY

19. Ghosh R, Aslam M, Kalita H. Graphene derivatives for chemiresistive gas sensors: A review. Materials Today Communications. 2022;30:103182.
20. Fan YY, Tu HL, Pang Y, Wei F, Zhao HB, Yang Y, et al. Au-decorated porous structure graphene with enhanced sensing performance for low-concentration NO_2 detection. Rare Metals. 2020;39(6):651-658.
21. Libeert G, Murugesan R, Guba M, Keijers W, Collienne S, Raes B, et al. Au_3-Decorated graphene as a sensing platform for O_2 adsorption and desorption kinetics. Nanoscale. 2022;14(34):12437-12446.
22. Suematsu K, Sasaki M, Ma N, Yuasa M, Shimanoe K. Antimony-Doped Tin Dioxide Gas Sensors Exhibiting High Stability in the Sensitivity to Humidity Changes. ACS Sensors. 2016;1(7):913-920.
23. Banerjee S, Bumajdad A, Devi PS. Nanoparticles of antimony doped tin dioxide as a liquid petroleum gas sensor: effect of size on sensitivity. Nanotechnology. 2011;22(27):275506.
24. Huang D, Yang Z, Li X, Zhang L, Hu J, Su Y, et al. Three-dimensional conductive networks based on stacked SiO_2 @ graphene frameworks for enhanced gas sensing. Nanoscale. 2017;9(1):109-118.
25. Shuai C, Yang F, Shuai Y, Peng S, Chen S, Deng Y, et al. Silicon dioxide nanoparticles decorated on graphene oxide nanosheets and their application in poly(l-lactic acid) scaffold. Journal of Advanced Research. 2023;48:175-190.
26. Liu Y, Ye C, Zhao H, Lin K, Cao X, Ai Y. Si-Doped Nitrogenated Holey Graphene (C_2N) as a Promising Gas Sensor for O-Containing Volatile Organic Compounds (VOCs) and Ammonia. Crystals. 2023;13(5):816.
27. Chen G, Gan L, Xiong H, Zhang H. Density Functional Theory Study of B, N, and Si Doped Penta-Graphene as the Potential Gas Sensors for NH_3 Detection. Membranes. 2022;12(1):77.
28. Zhang D, Jiang C, Liu J, Cao Y. Carbon monoxide gas sensing at room temperature using copper oxide-decorated graphene hybrid nanocomposite prepared by layer-by-layer self-assembly. Sensors Actuators B: Chem. 2017;247:875-882.
29. Panda D, Nandi A, Datta SK, Saha H, Majumdar S. Selective detection of carbon monoxide (CO) gas by reduced graphene oxide (rGO) at room temperature. RSC Advances. 2016;6(53):47337-47348.

CC BY